Unveiling the conformational landscape of achiral all- cis tert -butyl β-peptoids

Gaetano Angelici, Nicholus Bhattacharjee, Maxime Pypec, Laurent Jouffret, Claude Didierjean, Franck Jolibois, Lionel Perrin, Olivier Roy, Claude Taillefumier

ARTICLE

Unveiling the conformational landscape of achiral all-*cis tert*-butyl β-peptoids

Received 00th January 20xx,
Accepted 00th January 20xx

DOI: 10.1039/x0xx00000x

Gaetano Angelici,[a†‡] Nicholus Bhattacharjee,[bξ] Maxime Pypec,[a] Laurent Jouffret,[a] Claude Didierjean,[c] Franck Jolibois,[d] Lionel Perrin,[b] Olivier Roy,[a] and Claude Taillefumier*[a‡]

The synthesis and conformational study of *N*-substituted β-alanines with *tert*-butyl side chains is described. The oligomers prepared by submonomer synthesis and block coupling methods are up to 15 residues long and are characterised by amide bonds in the *cis*-conformation. A conformational study comprising experimental solution NMR spectroscopy, X-ray crystallography and molecular modeling shows that despite their intrinsic higher conformational flexibility compared to their α-peptoid counterparts, this family of achiral oligomers adopt preferred secondary structures including a helical conformation close to that described with (1-naphthyl)ethyl side chains but also a novel ribbon-like conformation.

Introduction

In the last few decades there has been a growing interest towards the study of peptoids (*N*-substituted glycines oligomers).[1] A lively and inquisitive peptoid scientific community was able to apply fundamental findings in the synthesis and conformational studies of these oligomers, for the discovery of new bioactive molecules[2] or for the development of new materials.[3] Peptoids, likewise peptides, show a dichotomous relationship between conformational structure and macroscopic properties, even though, the inherent absence of backbone hydrogen bond donors, confers to peptoids a higher flexibility. Peptoids' greater flexibility, as compared to peptides also originates from the isoenergetic character of the *cisoid* and *transoid* conformations of the tertiary amides linking the monomers.[4] Therefore, several side chains were engineered to bias the *cis*/*trans* equilibrium of the amide bond, in favour of *cis*[5] or *trans* isomers.[6] We have recently introduced the use of *tert*-butyl side chains (*t*Bu), which lock the amide bond in the *cis* conformation, for steric reasons, regardless of the solvent used.[7] The conformational properties of *t*Bu side chains-containing α-peptoids have been deeply studied showing that a combination of weak non-covalent interactions including *t*Bu--*t*Bu London dispersion forces promote helical folding of achiral *Nt*Bu peptoid homooligomers.[8] Moreover, the introduction of peptoid monomers carrying non-aromatic α-chiral side chains (*e.g.* *tert*-butylethyl group) in $(Nt\text{Bu})_n$ stretches allowed the formation of a stable all-*cis* PPI like helix.[9] *N*Cα-gem dimethyl side chains which can be seen as "functionalized" surrogates of the *tert*-butyl side chain have also been proposed.[10] The logical extension of the studies on *tert*-butyl all-*cis* peptoids was the synthesis and conformational analysis of their β-peptoid counterparts. β-Peptoids are peptidomimetics based on *N*-alkylated β-amino propionic acid residues.[11-17] They showed to have remarkable folding propensity, depending on the nature of the side chain, despite the presence of an additional methylene unit.[18-22] The strong ability of the *t*Bu side chain, to lock the *cis* isomer of the peptoid amide bond, coupled with the larger conformational space generally available in β-peptoids, led us toward the synthesis and extensive conformational analysis of the all-*cis* *tert*-butyl β-peptoids, as depicted in Figure 1. Their conformational preference has been explored through NMR spectroscopy, X-ray diffraction and molecular modelling. Two families of oligomers differing in their *C*-terminal group (ethyl ester or piperidinyl amide) were designed to increase our chances of obtaining singles crystals for X-ray diffraction studies (Figure 1).

[a] *Université Clermont Auvergne, Clermont Auvergne INP, CNRS, ICCF 63000 Clermont-Ferrand, France.*
[b] *Université de Lyon, Université Claude Bernard Lyon I, CNRS, INSA, CPE, UMR 5246, ICBMS, 1 rue Victor Grignard, F-69622 Villeurbanne, France*
[c] *Université de Lorraine, CNRS, CRM2, F-54000 Nancy, France*
[d] *Université de Toulouse-INSA-UPS, LPCNO, CNRS UMR 5215, 135 av. Rangueil, F-31077, Toulouse, France*

Corresponding Author
**E-mail:claude.taillefumier@uca.fr*

‡ Equal contributors
Present Address
† Dipartimento di Chimica e Chimica Industriale, Università di Pisa, Via G. Moruzzi 13, 56124 Pisa, Italy
ξ Department of Chemistry, University of Science & Technology Meghalaya, Ri-Bhoi, Meghalaya 793101

Electronic Supplementary Information (ESI) available: Experimental procedures, HPLC analytical data, NMR and IR spectra, full X-ray data for **1p**, **3p**, and **5a**, and computational data. See DOI: 10.1039/x0xx00000x
Compound **2p** (CCDC 2191892) (CIF)
Compound **3p** (CCDC 2191893) (CIF)
Compound **5a** (CCDC 2191995) (CIF)

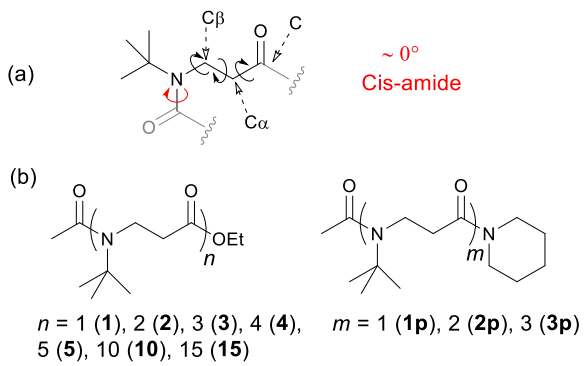

Figure 1. (a) Structure of a *tert*-butyl β-peptoid residue (β-N*t*Bu) showing a *cis* amide bond (ω) with the preceding (truncated) residue. The dihedral angles are specified in the drawing. (b) Synthesised molecules (for ease of drawing the amides are drawn in *trans*). Dihedral angles definition: ω [$C\alpha_{(i-1)}$; $C_{(i-1)}$; N; Cβ], φ [$C_{(i-1)}$; N; Cβ; Cα], θ [N; Cβ; Cα; C], ψ [Cβ; Cα; C; $N_{(i+1)}$].

Results and Discussion

Synthesis of *t*Bu β-peptoid oligomers

The shortest oligomers of the two families of molecules were synthesized in excellent yields, from ethyl acrylate (n = 1-5, Scheme 1) or piperidinyl acrylamide (m = 1-3, Scheme 2). The 1,4-addition of *tert*-butylamine to these starting building blocks resulted in the formation of monomers **1a** and **7**. These were then elongated through the classical submonomer approach in solution, consisting in building each new monomer by iteration of two steps, an acylation step of the *N*-terminus with acryloyl chloride followed by an aza-Michael reaction between the formed acrylamide compound and a primary amine, here *tert*-butylamine. The synthetic strategy in solution was preferred, as the aza-Michael step in supported synthesis, with this particularly hindered amine, was challenging.[8]

For the longest oligomers **10** (n = 10) and **15** (n = 15) we applied a previously optimized method,[8] based on a blockwise peptide coupling approach, using pentafluorophenyl activated esters as coupling partners. The activated esters were generated using either pentafluorophenyl diphenylphosphinate (FDPP) or pentafluorophenyl trifluoroacetate (TFAPfp) (Scheme 3). To our knowledge, the pentadecamer β-peptoid **15**, is the longest sequence-defined β-peptoid synthesised so far. A full description of the synthesis procedures for each molecule is given in the experimental section and Table 1 contains all purity data and mass spectrometry results that confirmed the identity of the compounds.

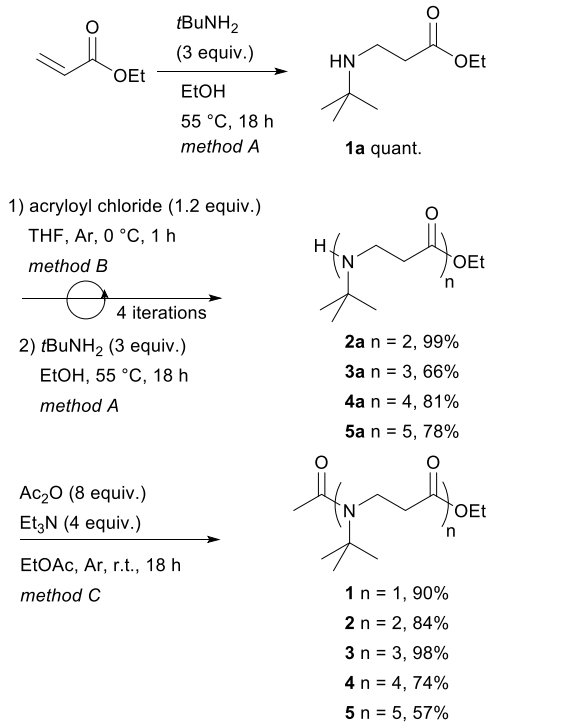

Scheme 1. Iterative submonomer synthesis of β-peptoids **1**, **2**, **3**, **4**, **5** with *C*-terminal ethyl ester (methods A-C are detailed in the Experimental Section).

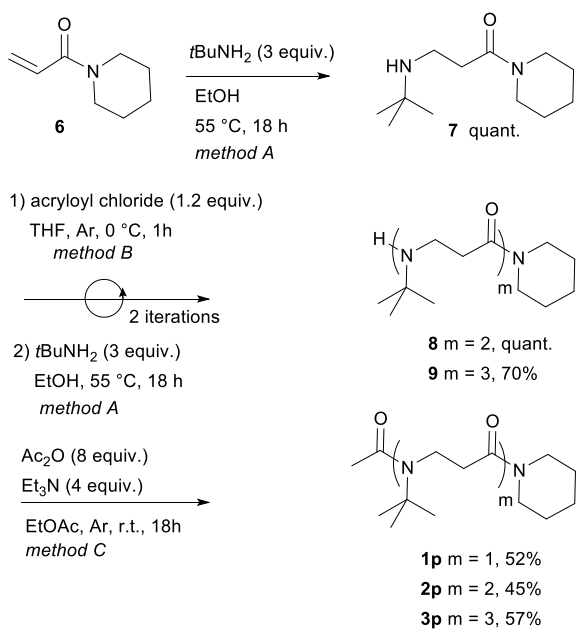

Scheme 2. Iterative submonomer synthesis of β-peptoids **1p, 2p** and **3p** with *C*-terminal piperidinyl amide (methods A-C are detailed in the Experimental Section).

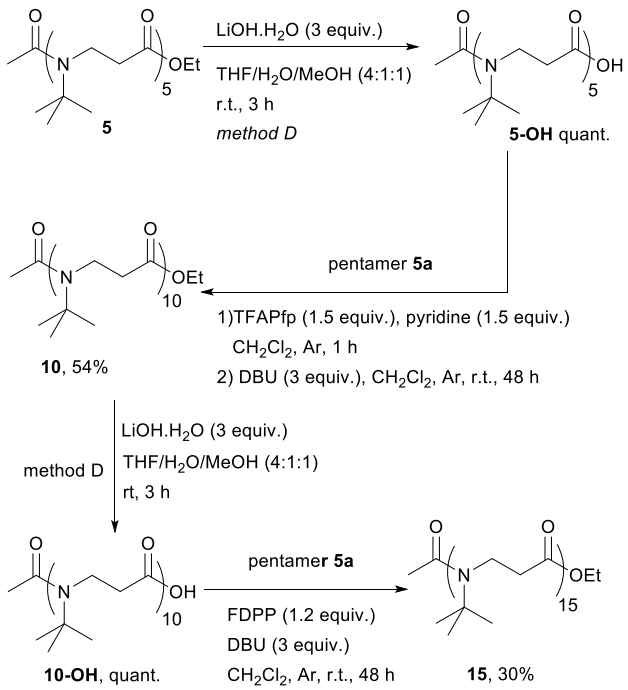

Scheme 3. Blockwise peptide coupling synthesis of β-peptoids **10** (n = 10) and **15** (n = 15).

Table 1. Sequences, purity, retention time, and calculated and observed masses for peptoids **1-5**, **10**, and **15**.

peptoid	sequence	% purity[a]	calc.mass	observed mass
1	Ac-β-*N*tBu-OEt	98.0	216.1594	216.1590 $[M+H]^+$
2	Ac-(β-*N*tBu)$_2$-OEt	100.0	343.2591	343.2589 $[M+H]^+$
3	Ac-(β-*N*tBu)$_3$-OEt	100.0	470.3588	470.3592 $[M+H]^+$
4	Ac-(β-*N*tBu)$_4$-OEt	97.4	597.4586	597.4591 $[M+H]^+$
5	Ac-(β-*N*tBu)$_5$-OEt	96.3	724.5583	724.5587 $[M+H]^+$
10	Ac-(β-*N*tBu)$_{10}$-OEt	92.4	1360.0568	1360.0579 $[M+H]^+$
15	Ac-(β-*N*tBu)$_{15}$-OEt	91.5	1995.5554	1995.5573 $[M+H]^+$
1p	Ac-β-*N*tBu-NPip	98.2	255.2067	255.2061 $[M+H]^+$
2p	Ac-(β-*N*tBu)$_2$-NPip	100.0	382.3064	383.3068 $[M+H]^+$
3p	Ac-(β-*N*tBu)$_3$-NPip	86.2	509.4061	509.4057 $[M+H]^+$

[a] Determined from the HPLC UV trace at 214 nm (conditions in ESI). "Pip" is the abbreviation for piperidinyl.

NMR Conformational studies

NMR spectroscopy was used to analyze the solution structures of peptoid monomers (**1**, **1p**), and dimers (**2**, **2p**) for which a broad dispersion of signals, in contrast to the longer oligomers, allowed an unambiguous assignment of the proton chemical shift from ^{1}H-^{1}H correlation spectroscopy (COSY).

In the tested solvents, $CDCl_3$, benzene-*d*6, and pyridine-*d*5, and CD_3CN we observed that the backbone methylene groups appeared as second order AA'XX' spin systems (400 MHz NMR spectrometer). As an example, representative J_{AX} and $J_{AX'}$ vicinal coupling constants of 5.2 and 11.0 Hz were calculated for momomer **1**. Enlargements of the second order multiplets of the backbone methylene have been included in the supplementary information for the monomers and dimers, as well as a breakdown of the AA'XX' spin system of monomer **1**.[23]. The larger coupling constant value is consistent with an extended conformation of the monomer backbone, i.e. with θ dihedral angles close to 180°. Two-dimensional NOESY experiments of monomers **1** and **1p**, and dimer **2p** confirmed that the *Nt*Bu amides are in the *cis* conformation. Figure 2 highlights the key NOE observed in dimer **2p**. The presence of a strong NOE between the acetyl-methyl and the backbone $^{\beta}CH_2$ protons (residue 1) indicates the presence of a *cis* amide bond at the *N*-terminal acetamide. Likewise, an NOE was observed between the $^{\beta}CH_2$ protons of residue 2 and the $^{\alpha}CH_2$ of residue 1, indicative of a *cis* amide bond between the two residues.

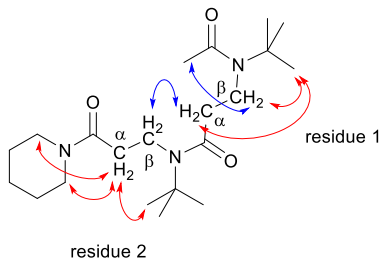

Figure 2. Key cross-peaks observed in the NOESY spectrum of dimer **2p** (shown as double-headed arrows). In blue the NOEs used to establish the *cis* conformation of the amide bonds.

Crystallographic analysis

We were able to obtain single crystals suitable for X-ray diffraction analysis of dimer **2p**, trimer **3p**, and pentamer ethyl ester **5a** from slow evaporation of solutions in ethyl acetate. The three oligomers crystallized in achiral space groups ($P2_1/c$ and P-1). Crystals of pentamer **5a**, dimer **2p** and trimer **3p** contain one, two and three independent molecules, respectively. The dihedral angles observed in the crystals are reported in Table 2. Small deviations from planarity of the amide bonds are observed (ω dihedral angles) and the values close to 0° unsurprisingly show that all the amides are in the *cis* conformation. Geometry optimizations at the DFT level[12] and experimental studies, including high-resolution X-ray crystallographic structures of β-peptoid oligomers with (*S*)-1-(1-naphthyl)ethyl side chains (s1npe), as reported by the Olsen group,[20] have shown that β-peptoids with *cis*-amide linkages can adopt a helical conformation with exactly three residues per turn and a helical pitch of 9.6-9.8 Å between turns.

Table 2. Dihedral angles in degrees of compounds **2p**, **3p**, and **5a**, as determined by X-ray crystallography. Out-of trend values are highlighted in red.

	Dimer 2p (conformation 1)				*Dimer 2p (conformation 2)*			
[a]*R*	*ω*	*φ*	*θ*	*ψ*	*ω*	*φ*	*θ*	*ψ*
1	1.2	-94.0	176.7	175.5	14.5	80.4	-170.5	168.0
2	-10.9	93.4	164.3	169.0	2.0	89.4	170.5	79.0
	Trimer 3p (conformer 1)				*Trimer 3p (conformer 2)*			
1	-6.0	-89.6	169.4	100.5	-9.8	-84.2	178.1	-172.9
2	-11.8	-92.5	173.1	-173.7	7.0	87.1	-152.4	163.5
3	1.6	88.4	178.5	164.9	9.5	-95.0	171.1	168.2
	Pentamer 5a				*Trimer 3p (conformer 3)*			
1	-	-	-	166.2	-3.6	-87.6	165.4	101.9
2	13.1	-99.2	164.1	85.4	-13.3	-90.9	171.7	-170.6
3	3.7	87.9	177.9	166.4	0.0	86.6	174.6	173.9
4	1.3	-94.8	-160.6	170.6				
5	-10.1	-81.9	171.5	-				

[a]Residue numbering.

Representative (φ, θ, ψ) dihedral angle values in the helical structure of the published hexamer Ac-(s1npe)$_6$-*t*Bu are (96.3°, 172.5°, -175.3°) as measured at residue 5. Most of the (θ, ψ) values in structures of **5a**, **1p** and **3p** agree with those described in the Olsen's work.[20] The θ angle values between ±165° and ±178° are also consistent with the measured vicinal coupling constants (~11 Hz) between the $^{\alpha}CH_2$ and $^{\beta}CH_2$ protons within the monomers, *i.e*. with monomers in extended conformation. A slight divergence can however be observed in the structure of **3p** (conformer 2) with θ = -152.4° for residue 2, and the ψ angle sometimes deviates from the ideal angle for a helical structure (~|178°|) with some values around |100°|. Concerning the φ angle values around 90-95°, they are also in line with those found in a helical structure but if we consider each structure individually, the signs of φ switch between positive and negative values (Figure 3). We can also observe that the positioning of the side chain methyl groups (which refers to the χ1 dihedral angle), is the same as that observed in the past for α-*Nt*Bu peptoid units, *i.e*. one of the Me group is roughly eclipsed with the N-$^{\beta}CH_2$ bond, which allows the other two Me groups to be positioned on either side of the carbonyl of the amide. To summarise, the units of β-*Nt*Bu oligomers adopt two main structures in the crystal state, a helix motif (φ = 90°, θ = 180°, ψ = 180°) and a turn motif (φ = 90°, θ = 180°, ψ = -100°). A propension to alternate handeness has been observed, which is not surprising since β-*Nt*Bu oligomers consist of achiral building blocks.

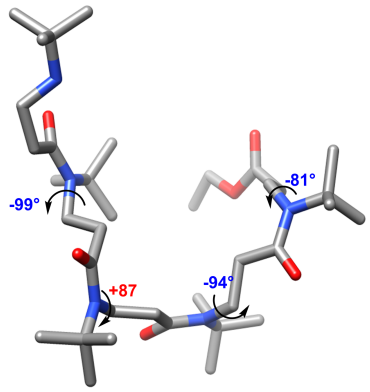

Figure 3. X-ray crystal structure of H-(β-*Nt*Bu)$_5$-OEt **5a** with the measured φ angles values. The hydrogen atoms have been omitted for clarity.

Computational analysis of β-*Nt*Bu peptoid oligomers

To elucidate further the conformational preference of β-*Nt*Bu petoid oligomers, we conducted molecular dynamics simulations and quantum mechanics calculations. More specifically, our objectives were to confirm the helical folding conformation observed in the crystal state, but also to identify possible alternative folding modes that could explain the angle values departing from a helical conformation.

Molecular Dynamics simulations

Molecular Dynamics simulations were performed using NAMD software package[24] and the Generalized AMBER Force Field (GAFF) parameters[25] to describe the potential of β-*Nt*Bu peptoid monomers. Fully detailed computational procedures are available in the ESI. 50 ns classical molecular dynamics simulations were performed on octamer and 16-mer compounds solvated in acetonitrile box with a buffer of 16Å towards each direction. The oligomers were capped with an acetyl group at the *N*-terminus and as a dimethylamide at the *C*-terminus. The dihedral angles extracted from the crystals were used to construct the starting structures (φ = ±90°, θ = 180°, ψ = 180°) with the exception of the ω amide bond which was set in *trans*. Two particular patterns were then studied for each oligomer length, one keeping the sign of φ angle constant, denoted $(+)_x$, and another one in which the sign of φ alternates along the sequence, denoted $(+/-)_y$. Conversion of ω dihedral angle from *trans* to *cis* was observed during initial production runs of 10 ns. Figures S1-S4 show RMSD and end-to-end distances during the simulations. Fluctuation of RMSD is slightly higher for the $(+)_8$ and $(+)_{16}$ structures relative to the alternate $(+/-)_4$ and $(+/-)_8$. The end-to-end distance fluctuates between 10-30 Å for octamer and 20-55 Å for 16-mer. These large fluctuations reflect the high flexibility of β-peptoids with conformations ranging from extended chain to helical structure and to turns.

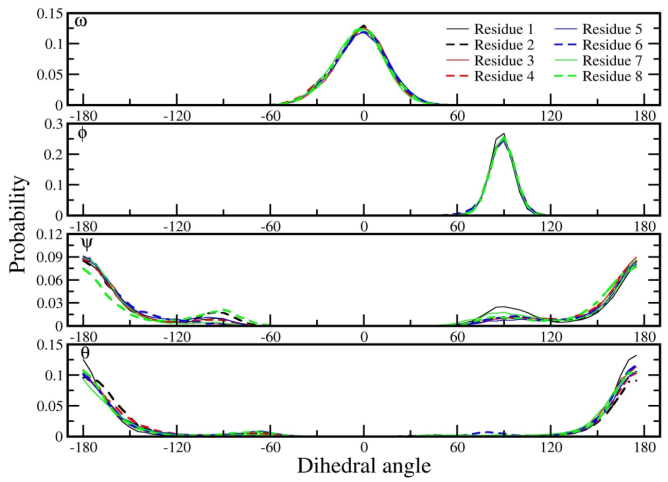

Figure 4. Probability distribution of dihedral angles from 50 ns simulation of $(+)_8$ β-*Nt*Bu octapeptoid.

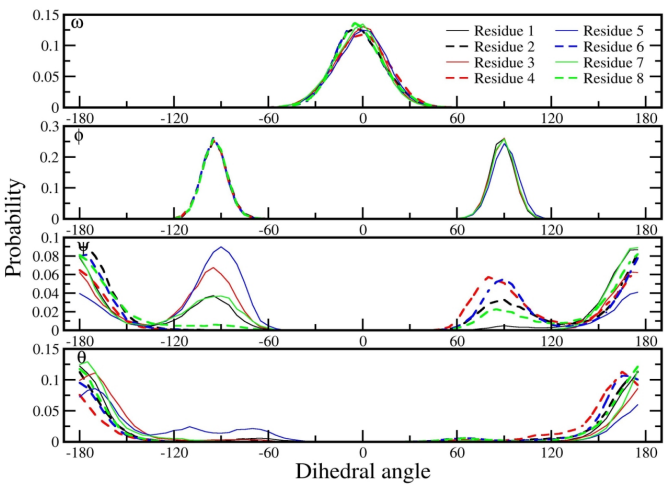

Figure 5. Probability distribution of dihedral angles from 50 ns simulation of $(+/-)_4$ β-*Nt*Bu-octapeptoid.

Figures 4 and 5 show the distribution probability of dihedral angles during the simulation of the $(+)_8$ and $(+/-)_4$ octamers (for 16-mers $(+)_{16}$ and $(+/-)_8$, see Figures. S5 and S6 in the ESI).
The peptoid amide bond shows a prevalence for the *cis* conformation in all simulations. Only one deviation was observed, between residues 9 and 10 in the case of the 16-mer $(+/-)_8$ (~10% of the simulation time). Distribution of φ angle values are narrow with values centred around +90° for the $(+)_8$ and $(+)_{16}$ structures and ±90° for the alternate $(+/-)_4$ and $(+/-)_8$ conformation. The most interesting feature concerns the ψ angle distribution. For $(+)_8$ octamer, the ψ angle distribution is centred around ±170° with a slight population at ±90° (~6%). However, for the $(+/-)_4$ octamer, the population at ±90° increases considerably and becomes equivalent to that at ±170°. The possibility of β-peptoids having ψ angle values of ±85 was previously reported based on *ab initio* molecular modelling studies.[12] Lastly, whatever the conformational pattern $(+)_x$ or $(+/-)_y$, the θ angle originating from the additional β-carbon in the main chain of β-peptoids, is found to spread around ±170°. Similar results are observed for the 16-mer $(+)_{16}$ and $(+/-)_8$ as shown in Figures S5 and S6 of the ESI.

The results of this modelling contribution can be summarised as follows: distributions of dihedral angles obtained by molecular dynamics of the $(+)_n$ oligomers are consistent with helical structures. In the case of the alternate $(+/-)_m$ oligomers, a new regular folding mode is evidenced. This new conformation is characterised by φ and ψ angles close to |90°|, whose signs alternate from one residue to another. The signs of the (φ,ψ) angles are also opposite within a monomer (Figure 5).
To enhance the conformational sampling during molecular dynamics simulations, Replica Exchange Molecular Dynamics (REMD) simulations were also performed on the $(+)_8$ and $(+/-)_4$ octamers (Figures S7 and S8, ESI). These simulations were performed for a temperature range of 300 to 600K, and each replica was simulated for 50 ns as described in a previous communication.[8] Trajectory analyses reveal an equal probability of switch of sign for the φ angle for the $(+)_8$ and $(+/-)_4$ conformations. This contrasts from the case of the *Nt*Bu α-peptoids for which a very limited switch of sign of φ was observed for the $(+)_8$ octamer. This conformer was also computed more stable relative to the alternate one in the case of *Nt*Bu α-peptoids. This also illustrates the higher flexibility of β-peptoids relative to α-peptoids. The monitoring of the amide torsion (ω) of β-peptoids also display a larger fluxionality than that of α-peptoids. In α-peptoids, the amide bonds remain in *cis* even at high temperature during REMD simulation. REMD simulations of both $(+)_8$ and $(+/-)_4$ β-peptoid conformers reveal that all peptoid amide bonds isomerize from *cis* to *trans* for a significant amount of simulation time.

Quantum Chemical Calculations.

In order to refine conformational parameters, $(+)_n$ and $(+/-)_m$ tetramers and hexamers have been fully optimized at the DFT level using the B3LYP density functional. Solvation by chloroform was represented during the optimization by an implicit model. using Before optimization, structures were built-up using GaussView.[26] Each peptoid was capped at the *N*-terminus with an acetyl group and an ethyl ester was set at the *C*-terminus. The ω torsions were set in the *cis* conformation and the θ torsions at 180°. Then two conformational patterns were considered, the first one with (φ,ψ) = (+90°, 180°) and the second one with both φ and ψ angles set at ±90°, with φ and ψ opposite in sign within a monomer and alternating along the sequence, as observed in MD simulations.
The fully optimized structure of the (φ,ψ) = (+90°, 180°) conformational pattern is helical, as shown at the hexamer length in Figure 6A (torsion angles are provided in Table S3). The helix features 2.75 residues per turn and a helical pitch of 8.5 Å, which is slightly different from the known *N*s1npe β-peptoid that displays a triangular-prism-shaped helix with 3 residues per turn and a pitch of 9.9 Å.[20]

Table 3 reports the optimized torsions for the (+/-)-hexamer as a representative example of the folding of the (+/-) alternating oligomers (torsions angles of the tetramer in Table S4). The six residues in the structure adopt approximately the same conformation, which exists in two alternating mirror-image forms along the sequence. This results in a unique discrete

secondary structure consisting of a repetition of turn units, which together form a ribbon-like structure (Figure 6C) with a master curved shape (Figure 6D). The curved ribbon can be approximated by two straight segments corresponding to residues 1-3 and 3-6, with a bend of ≈ 50°. The (+/-)-model dimer is the shortest peptoid that can adopt one full unit of the ribbon-type structure. A reverse turn of the backbone is then generated with each new addition of monomer, which lengthens the ribbon-like structure by about 5.8 Å ($N^{i}...CO^{i+1}$ distance). It should be noted that the discovery of a peptoid ribbon secondary structure was first reported in 2013 and involved an α-peptoid backbone with alternating *cis*- and *trans*-amide bonds.[27]

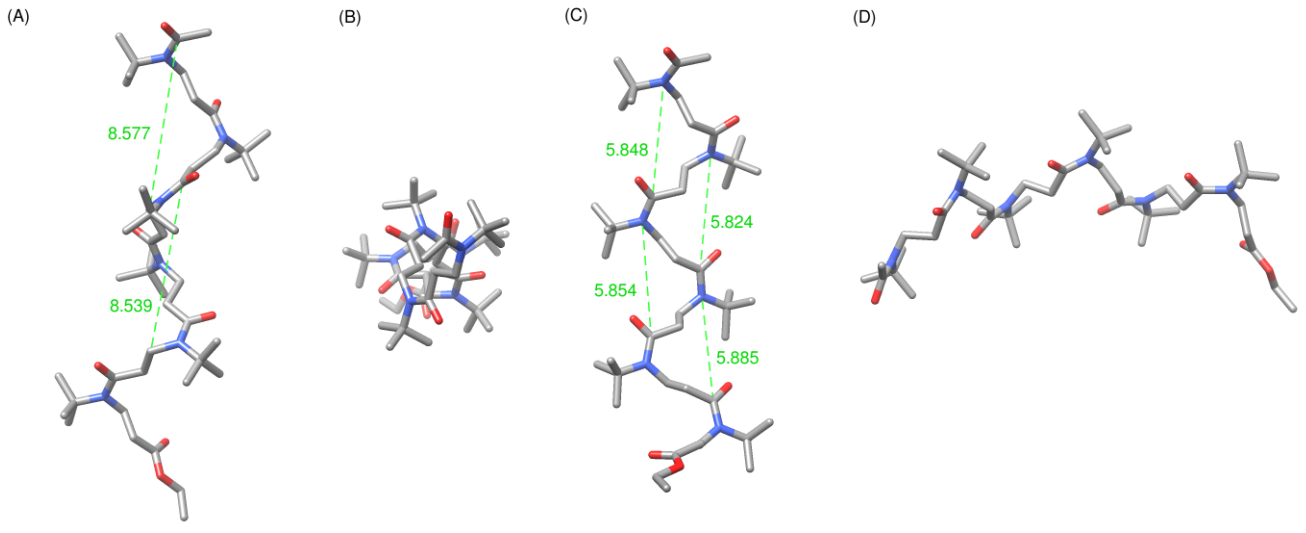

Figure. 6. Optimized structures at the DFT level of all-(+) and (+/-) hexamers. (A/B) Helical structure of all-(+) model hexamer (Ac-(β-*Nt*Bu)$_6$-OEt), (A) view perpendicular to the helical axis, (B) Top view along the helical axis. (C/D) Ribbon-like structure of (+/-) model hexamer (Ac-(β-*Nt*Bu)$_6$-OEt), (C) view perpendicular to the ribbon plane, (D) side view showing the curved shape.

Table 3. Optimized torsions of (+/-)-peptoid Ac-(β-*Nt*Bu)$_6$-OEt

residue	ω	φ	θ	ψ
1	9.80	84.82	-158.30	-103.14
2	-0.94	-85.23	160.98	108.39
3	-0.90	85.31	-159.60	-115.12
4	5.58	-86.44	160.25	112.58
5	-2.26	85.08	-160.85	-110.85
6	3.82	-87.93	164.03	

Quantifying weak non-covalent interactions.

As previously reported regarding the conformational analysis of *Nt*Bu α-peptoids, weak interactions were shown to stabilize helix formation. The occurrence of interactions such as (i) CO(i)…HC(j) hydrogen bond along the backbone and (ii) London attractive force between *t*Bu side chains has been counted along a trajectory based in distance criteria.[8] Similarly, this analysis has been performed for the β-peptoids under study.

In sharp contrast to *Nt*Bu α-peptoids either none or negligible amounts of backbone CH…O=C interactions are observed during the simulations, considering both the α-, and β-methylene groups. However, the side chains methyl groups form significant amount of weak CH…O=C hydrogen bond in both (+)$_8$ and (+/-)$_4$ conformations (Figures S9 and S10, ESI). These interactions are observed only between the C=O of residues *i* and methyl side chains of residues *i+1*, not with the methyl side chains of *i-1* residues, as in the case of *Nt*Bu α-peptoids. Overall, this stabilizing interaction does not provide an advantage of one conformation over the other as it is found with approximately the same probability for both (+)$_8$ and (+/-)$_4$ model peptoids.

Concerning intramolecular London interaction between *tert*-butyl side chains, their probability was found lower for β-peptoids than for their α-counterparts. However, the (+/-) oligomers have a slightly higher tendency of forming i/i+2 side chain London interactions in comparison to the all-(+) oligomers for which i/i+3 *t*Bu side chain interactions are more pronounced (Figure S11). On the overall, based on molecular dynamics simulation, no conformation selectively displays a large amount of weak intramolecular interactions. This agrees with the overall flexibility of β-peptoids and is further supported by the small energy difference of 2 to 5 kcal mol^{-1} at the DFT level between the (+) and (+/-) optimised structures.

Conclusions

Various strategies for controlling peptoid conformation involving steric and electronic interactions between peptoid amides and nearby side chains have been developed in recent years. In contrast, β-peptoids which are more difficult to fold into discrete secondary structures than their α-counterparts have been sparsely studied and in fact only the use of the (1-naphthyl)ethyl side chain had so far allowed the formation of stable secondary structures, with a helical display. Here, we have exploited the *cis*-amide promoting effect of the aliphatic sterically-hindered *tert*-butyl side chain to help folding of β-peptoid oligomers. The target β-*Nt*Bu oligomers with length up to 15 residues were synthesized using submonomer and block-coupling approaches. 2-D NOESY experiments confirmed the

cisoid conformation of the *β-Nt*Bu amide bonds for the monomers and dimers. This was further evidenced by X-ray diffraction analysis of three peptoid structures. In addition, an extended conformation of the monomer units was determined by NMR and in the crystal state and recovered by MD simulations. The simulations not only confirmed the known fact that *β*-peptoids are more flexible, they also provided a better understanding of the folding and dynamic of these achiral peptidomimetic oligomers with no aromatic side chains.

A helix structure with approximately three residues per turn as already described in the literature[20] was revealed by classical MD but at higher temperature, REMD simulation revealed a new ribbon-like regular structure characterized by dihedral angles ($\varphi \approx 85°$, $\theta \approx 160°$, $\psi \approx -110°$) and whose signs alternate from one residue to another. Our aim is now to implement strategies that could contribute to the stabilization of this ribbon structure. In particular, we are currently investigating site-specific replacement of terbutylic side chains with *cis*-amide inducing functional *N*Cα gem-dimethyl side chains and/or chiral *cis*-amide inducing side chains.[10]

Experimental section

Chemicals obtained from commercial sources were used without further purification unless stated otherwise. Ethyl acrylate, Acryloyl chloride, Tert-butylamine (98% purity), Pentafluorophenyl diphenylphosphinate (FDPP), Pentafluorophenyl trifluoroacetate (TFAPfp), 1,8-Diazabicyclo[5.4.0]undec-7-ene (DBU), were purchased from Sigma-Aldrich, MC2 France. Piperidine (99% purity) was purchased from Avocado, France. THF, CH_2Cl_2, and MeOH were dried over aluminum oxide via a solvent purification system and stored over 4 Å molecular sieves. EtOAc, CH_2Cl_2, cyclohexane, and MeOH for column chromatography were obtained from commercial sources and were used as received. Et_3N was dried over KOH, distilled and stored over 4 Å molecular sieves.

General procedures of the repetitive synthetic strategies are reported below, while the experimental details of each synthesised compound are available in the supporting information.

Method A (aza-Michael reactions)

To a solution of α,β-unsaturated amide in Ethanol (1M) at 0°C, three equivalents of primary amine were added. The solution was stirred overnight at 55°C, in reflux. Reaction was monitored by TLC. If reaction was not complete, other 2 equivalents of primary amine were added and let stirring until complete conversion. *t*-Butyl amine is volatile enough to be distilled under reduced pressure, to obtain a crude used in the next step, without further purification needed.

Method B (acetylation of secondary amines with acryloyl chloride)

Secondary amine (1 equiv.) was dissolved in dry THF under Argon (0.25 M) and cooled down to 0°C with an ice bath. Et_3N (1.2 equiv.) was added and acryloyl chloride (1.2 equiv.) was slowly dropped into the flask. The solution was let stirring for 1h at 0°C. The resulting slurry solution was filtered and concentrated under reduced pressure. The crude was purified by flash chromatography.

Method C (acetylation of secondary amines with acetic anhydride)

Secondary amine (1 equiv.) was dissolved in dry ethyl acetate (0.20 M) and added with Et_3N (4 equiv.). Acetic anhydride (8 equiv.), was slowly dropped in the flask, and the reaction was let stirring overnight at room temperature. The solution was diluted with ethyl acetate and subsequently washed with an aqueous solution of HCl (1N) and a saturated solution of $NaHCO_3$. The organic fraction was dried over sodium sulfate and concentrate under reduced pressure, to give the crude product. Products were purified and isolated by column chromatography.

Method D (saponification of ethyl esters)

Ethyl ester (1 equiv.) was dissolved in a mixture of THF/H_2O/MeOH, 4:1:1 (0.25M), and added with LiOH (3 equiv.). Solution was let stirring at room temperature for 3h. Reaction was monitored by TLC, until complete conversion. The resulting solution was diluted with Ethyl acetate and washed with an aqueous solution of HCl (1N). The organic fraction was dried over sodium sulfate and concentrate under reduced pressure, to give the crude product without any further purifications.

Monomer 1: Rf = 0.44 (cyclohexane/EtOAc 50:50); ^{1}HNMR (400 MHz, $CDCl_3$) *δ* (ppm): 1.27 (t, *J* = 7.1 Hz, 3H), 1.44 (s, 9H), 2.14 (s, 3H), 2.56 (m, 2H), 3.63 (m, 2H), 4.15 (q, *J* = 7.1 Hz, 2H); ^{13}C NMR (100 MHz, $CDCl_3$) *δ* (ppm): 14.2, 24.9, 29.0, 36.4, 42.0, 57.2, 60.8, 171.0, 171.4; HRMS (TOF MS ES+): calcd for $C_{11}H_{22}NO_3$ [M + H]+ m/z 216.1594, found 216.1590.

Dimer 2: Mp = 52°C; Rf = 0.40 (cyclohexane/EtOAc 50:50); IR (ATR) ν (cm^{-1}): 2978, 2964, 1726, 1637, 1477, 1450, 1357, 1344, 1317, 1223, 1178, 1148, 1028, 1004; ^{1}H NMR (400 MHz, benzene-*d*6) δ 3.89 (q, *J* = 7.1 Hz, 2H), 3.64 – 3.56 (m, 2H), 3.37 – 3.28 (m, 2H), 2.46 – 2.38 (m, 2H), 2.27 – 2.19 (m, 2H), 1.99 (s, 3H), 1.44 (s, 9H), 1.29 (s, 9H), 0.93 (t, *J* = 7.1 Hz, 3H). ^{1}H NMR (400 MHz, Pyr-*d*5) δ 4.13 (q, *J* = 7.1 Hz, 2H), 3.85 (m, 4H), 2.97 – 2.85 (m, 2H), 2.84 – 2.74 (m, 2H), 2.23 (s, 3H), 1.53 (d, *J* = 7.3 Hz, 18H), 1.15 (t, *J* = 7.1 Hz, 3H). ^{13}C NMR (101 MHz, $CDCl_3$) δ 171.3, 170.8, 170.5, 60.9, 57.4, 56.9, 42.7, 40.7, 37.3, 36.6, 28.9 25.0, 14.16. HRMS (TOF MS ES+): calcd for $C_{18}H_{35}N_2O_4$ [M + H]$^+$ *m/z* 343.2591, found 343.2589.

Trimer 3: ^{1}H NMR (400 MHz, $CDCl_3$) δ 4.15 (q, *J* = 8 Hz, 2H), 3.62 (m, 6H), 2.64 – 2.48 (m, 6H), 2.13 (s, 3H), 1.47 – 1.39 (m, 27H), 1.27 (t, *J* = 8 Hz, 3H). ^{1}H NMR (400 MHz, benzene-*d*6) δ 3.92 (q, *J* = 7.1 Hz, 2H), 3.74 – 3.59 (m, 4H), 3.38 – 3.28 (m, 2H), 2.62 – 2.49 (m, 4H), 2.27 – 2.19 (m, 2H), 2.05 (s, 6H), 1.47 (s, 9H), 1.43 (s, 9H), 1.27 (s, 9H), 0.96 (t, *J* = 7.1 Hz, 3H). ^{1}H NMR (400 MHz, Pyr-*d*5) δ 4.14 (q, *J* = 7.1 Hz, 2H), 3.99 – 3.91 (m, 2H), 3.91 – 3.80 (m, 4H), 3.02 – 2.90 (m, 4H), 2.82 – 2.74 (m, 2H), 2.25 (s, 3H), 1.55 (d, *J* = 3.8 Hz, 18H), 1.50 (s, 9H). ^{13}CNMR

(100 MHz, $CDCl_3$) δ (ppm): 14.1, 28.9, 29.0, 36.3, 37.5, 40.7, 41.5, 42.9, 57.3, 57.5, 61.0, 170.4, 170.6, 171.0. HRMS (TOF MS ES+): calcd for $C_{25}H_{48}N_3O_5$ $[M + H]^+$ *m/z* 470.3588, found 470.3592

Tetramer 4: Rf = 0.40 (cyclohexane/EtOAc 30:70); IR (ATR) ν (cm^{-1}): 2974, 2928, 1723, 1639, 1479, 1450, 1395, 1364, 1290, 1188, 1146, 1065, 1020, 928; ^{1}H NMR (400 MHz, benzene-*d*6) δ (ppm): 3.93 (q, *J* = 7.1 Hz, 2H), 3.77 – 3.60 (m, 6H), 3.41 – 3.32 (m, 2H), 2.69 – 2.58 (m, 4H), 2.58 – 2.50 (m, 2H), 2.31 – 2.22 (m, 2H), 2.08 (s, 3H), 1.53 – 1.37 (m, 27H), 1.28 (s, 9H), 0.96 (t, *J* = 7.1 Hz, 3H). ^{13}CNMR (100 MHz, $CDCl_3$) δ (ppm): 14.1, 24.9, 28.9, 29.0, 36.6, 37.5, 40.7, 42.9, 57.0, 57.2, 57.4, 57.5, 60.9, 170.4, 170.5, 170.0, 171.4. HRMS (TOF MS ES+): calcd for $C_{32}H_{61}N_4O_6$ $[M + H]^+$ *m/z* 597.4586 found 597.4591

Pentamer 5: Rf = 0.30 (cyclohexane/EtOAc 30:70); IR (ATR) ν (cm^{-1}): 2967, 2916, 1732, 1639, 1479, 1450, 1395, 1362, 1290, 1207, 1186, 1146, 1065, 1018, 928, 905. ^{1}H NMR (400 MHz, $CDCl_3$) δ 4.14 (q, *J* = 7.1 Hz, 2H), 3.65 – 3.59 (m, 10H), 2.66 – 2.48 (m, 10H), 2.13 (s, 3H), 1.49 – 1.36 (m, 45H), 1.26 (t, *J* = 7.1 Hz, 3H). ^{13}CNMR (100 MHz, $CDCl_3$) δ (ppm): 14.1, 24.9, 29.0, 36.7, 37.7, 40.7, 41.5, 43.0, 57.0, 57.4, 57.5, 61.0, 170.4, 170.6, 171.6; HRMS (TOF MS ES+): calcd for $C_{39}H_{74}N_5O_7$ $[M + H]^+$ *m/z* 724.5583 found 724.5587

Decamer 10: Mp = 155°C; Rf = 0.20 (cyclohexane/EtOAc 30:70); IR (ATR) ν (cm^{-1}): 2972, 2926, 1734, 1647, 1630, 1481, 1404, 1360, 1257, 1192, 1148, 1064, 1014; ^{1}H NMR (400 MHz, $CDCl_3$) δ 4.16 (q, *J* = 7.1 Hz, 2H), 3.65 – 3.60 (m, 20H), 2.69 – 2.48 (m, 20H), 2.14 (s, 3H), 1.50 – 1.37 (m, 90H), 1.27 (t, *J* = 7.1 Hz, 3H). ^{13}CNMR (100 MHz, $CDCl_3$) δ (ppm): 14.1, 24.9, 28.9, 36.6, 37.5, 37.7, 40.6, 41.5, 42.9, 57.0, 57.3, 57.5, 60.9, 170.3, 170.5, 171.5; HRMS (TOF MS ES+): calcd for $C_{74}H_{139}N_{10}O_{12}$ $[M + H]^+$ *m/z* 1360.0568, found 1360.0579

Pentadecamer 15: Mp = 198°C; Rf = 0.10 (cyclohexane/EtOAc 30:70); IR (ATR) ν (cm^{-1}): 2967, 2928, 2889, 1734, 1647, 1630, 1481, 1456, 1400, 1360, 1192, 1148, 1069, 1013; ^{1}H NMR (400 MHz, CD_2Cl_2) δ 4.12 (q, *J* = 7.1 Hz, 2H), 3.68 – 3.52 (m, 30H), 2.68 – 2.47 (m, 30H), 2.08 (s, 3H), 1.41 (d, *J* = 1.8 Hz, 135H), 1.24 (t, *J* = 7.1 Hz, 3H). ^{13}CNMR (100 MHz, CD_2Cl_2) δ (ppm): 14.4, 25.2, 29.1, 38.3, 41.1, 42.0, 57.1, 57.5, 57.7, 170.8, 170.9, 171.0; HRMS (TOF MS ES+): calcd for $C_{109}H_{204}N_{15}O_{17}$ $[M + H]^+$ *m/z* 1995.5554 found 1995.5573

Monomer 1p: Rf = 0.24 (cyclohexane/EtOAc 20:80); ^{1}HNMR (400 MHz, $CDCl_3$) *δ* (ppm): 1.45 (s, 9H), 1.58 (m, 4H), 1.65 (m, 2H), 2.13 (s, 3H), 2.53 (m, 2H), 3.39 (m, 2H), 3.55 (m, 2H), 3.67 (m, 2H); ^{13}C NMR (100 MHz, $CDCl_3$) *δ* (ppm): 24.5, 25.1, 25.5, 26.5, 29.2, 34.7, 42.6, 46.5, 57.0, 168.4, 171.4; HRMS (TOF MS ES+): calcd for $C_{14}H_{27}N_2O_2$ $[M + H]+$ *m/z* 255.2067, found 255.2061.

Dimer 2p: Mp = 87°C; Rf = 0.30 (EtOAc 100%); IR (ATR) ν (cm^{-1}): 2930, 2858, 1633, 1442, 1393, 1295, 1290, 1276, 1271, 1248, 1003; ^{1}H NMR (400 MHz, $CDCl_3$) δ 3.70 – 3.59 (m, 4H), 3.59 – 3.51 (m, 2H), 3.42 – 3.33 (m, 2H), 2.62 – 2.45 (m, 4H), 2.14 (s, 3H), 1.71 – 1.62 (m, 2H), 1.58 (m, 4H), 1.44 (d, *J* = 1.0 Hz, 18H). ^{1}H NMR (500 MHz, benzene-*d*6) δ 3.64 (td, *J* = 10.4, 8.0 Hz, 4H), 3.41 (s, 2H), 2.82 – 2.73 (m, 2H), 2.55 – 2.45 (m, 2H), 2.33 – 2.23 (m, 2H), 2.00 (s, 3H), 1.44 (s, 9H), 1.39 (s, 9H). ^{1}H NMR (500 MHz, Pyr-*d*5) δ 3.95 (dd, *J* = 8.9, 6.6 Hz, 2H), 3.91 – 3.84 (m, 2H), 3.62 – 3.55 (m, 2H), 3.38 – 3.28 (m, 2H), 2.96 – 2.88 (m, 2H), 2.85 – 2.78 (m, 2H), 2.24 (s, 3H), 1.55 (s, 9H), 1.53 (s, 9H), 1.38 (m, 6H). ^{13}CNMR (100 MHz, $CDCl_3$) δ (ppm): 24.2, 24.9, 25.3, 26.3, 28.9, 34.7, 37.2, 41.3, 42.5, 42.7, 46.3, 56.9, 57.2, 167.7, 170.8, 171.2; HRMS (TOF MS ES+): calcd for $C_{21}H_{40}N_3O_3$ $[M + H]^+$ *m/z* 382.3064, found 382.3068.

Trimer 3p: Rf = 0.20 (cyclohexane/EtOAc 30:70); IR (ATR) ν (cm^{-1}): 2939, 2856, 1634, 1436, 1394, 1360, 1291, 1269, 1184, 1140, 1003; ^{1}H NMR (400 MHz, $CDCl_3$) δ 3.65 (m, 6H), 3.58 – 3.52 (m, 2H), 3.41 – 3.34 (m, 2H), 2.58 (dd, *J* = 9.3, 6.7 Hz, 4H), 2.54 – 2.47 (m, 2H), 2.14 (s, 3H), 1.64 (dd, *J* = 8.1, 5.2 Hz, 6H), 1.48 – 1.39 (m, 27H). ^{1}H NMR (400 MHz, Pyr) δ 4.01 – 3.92 (m, 4H), 3.88 (m, 2H), 3.63 – 3.55 (m, 2H), 3.39 – 3.33 (bs, 2H), 3.06 – 2.90 (m, 4H), 2.81 (m, 2H), 2.25 (s, 3H), 1.60 – 1.48 (m, 27H), 1.40 – 1.36 (m, 6H). ^{13}CNMR (100 MHz, $CDCl_3$) δ (ppm): 24.3, 24.9, 25.3, 26.4, 26.8, 34.7, 37.3, 37.4, 41.3, 41.5, 42.6, 42.9, 46.4, 57.0, 57.3, 65.7, 167.8, 170.5, 170.9, 171.5; HRMS (TOF MS ES+): calcd for $C_{28}H_{53}N_4O_4$ $[M + H]^+$ *m/z* 509.4061 found 509.4057

Acknowledgements

This work was supported by a grant overseen by the French National Research Agency project ARCHIPEP. LP and NB thank the CCIR of ICBMS and P2CHPD of Univ. Lyon 1 for providing computational resources. NB and FJ thank the CALcul en Midi-Pyrénées (CALMIP, grant P0758) for generous allocations of computer time. CT thanks M. Leremboure for mass spectrometry (UCA PARTNER) and Aurélie Job for HPLC analysis. NB also acknowledges SERB-DST, India for funding (SRG/2020/001543). The authors thank the PMD²X X-ray diffraction facility of the Institut Jean Barriol, Université de Lorraine, for single crystal X-ray diffraction measurements.

Conflicts of interest

There are no conflicts to declare.

References

1 (a) R. J. Simon, R. S. Kania, R. N. Zuckermann, V. D. Huebner, D. A. Jewell, S. Banville, S. Ng, L. Wang, S. Rosenberg, C. K. Marlowe, D. C. Spellmeyer, R. Tan, A. D. Frankel, D. V. Santi, F. E. Cohen, P. A. Bartlett, *Proc. Natl. Acad. Sci. U. S. A.* 1992, **89**, 9367. (b) R. N. Zuckermann, *Biopolymers*, 2011, **96**, 545.

2 (a) R. N. Zuckermann, T. Kodadek, *Curr. Opin. Mol. Ther.* 2009, **11**, 299. (b) S. A. Fowler and H. E. Blackwell, *Org. Biomol. Chem.*, 2009, **7**, 1508. (c) W. S. Horne, *Exp. Opin. Drug Discov.* 2011**, 6** , 1247. (d) M. T. Dohm, R. Kapoor, A. E. Barron, *Curr. Pharm. Des.,* 2011, **17** , 2732. (e) A. S. Culf, *Biopolymers*, 2019, e23285.

3 (a) J. Sun and R. N. Zuckermann, *ACS Nano*, 2013, **7**, 4715.

(b) K. H. A. Lau, *Biomater. Sci.*, 2014, **2**, 627. (c) C. Secker, S. M. Brosnan, R. Luxenhofer and H. Schlaad, *Macromol. Biosci.*, 2015, **15**, 881. (d) A. S. Knight, E. Y. Zhou, M. B. Francis and R. N. Zuckermann, *Adv. Mater.*, 2015, **27**, 5665. (e) N. Gangloff, J. Ulbricht, T. Lorson, H. Schlaad and R. Luxenhofer, *Chem. Rev.*, 2016, **116**, 1753. (f) A. Battigelli, *Biopolymers*, 2019, **110**, e23265. (g) S. Xuan and R. N. Zuckermann, *Polymer (Guildf).*, 2020, **202**, 122691.

4 (a) Q. Sui, D. Borchardt, D. L. Rabenstein, *J. Am. Chem. Soc*., 2007, **129**, 12042. (b) G. L. Butterfoss, P. D. Renfrew, B. Kuhlman, K. Kirshenbaum and R. Bonneau, *J. Am. Chem. Soc.*, 2009, **131**, 16798. (c) B. C. Gorske, J. R. Stringer, B. L. Bastian, S. A. Fowler, H. E. Blackwell, H. E. *J. Am. Chem. Soc*., 2009, **131**, 16555. (d) B. C. Gorske, R. C. Nelson, Z. S. Bowden, T. A. Kufe and A. M. Childs, *J. Org. Chem.*, 2013, **78**, 11172. (e) D. Kalita, B. Sahariah, S. Pravo Mookerjee, B. Kanta Sarma, *Chem. Asian J.,* 2022, **17**, e202200149.

5 (a) K. Kirshenbaum, A. E. Barron, R. A. Goldsmith, P. Armand, E. K. Bradley, K. T. V. Truong, K. A. Dill, F. E. Cohen, R. N. Zuckermann, *Proc. Natl. Acad. Sci. USA*, 1998, **95**, 4303. (b) C. W. Wu, K. Kirshenbaum, T. J. Sanborn, J. A. Patch, K. Huang, K. A. Dill, R. N. Zuckermann, A. E. Barron, *J. Am. Chem. Soc*., 2003, **125**, 13525. (c) B. C. Gorske, B. L. Bastian, G. D. Geske and H. E. Blackwell, *J. Am. Chem. Soc.*, 2007, **129**, 8928. (d) J. R. Stringer, J. A. Crapster, I. a. Guzei and H. E. Blackwell, *J. Am. Chem. Soc.*, 2011, **133**, 15559. (e) C. Caumes, O. Roy, S. Faure and C. Taillefumier, *J. Am. Chem. Soc.*, 2012, **134**, 9553. (f) A. A. Fuller, B. A. Yurash, E. N. Schaumann, F. J. Seidl, *Org. Lett*. 2013, **15**, 5118. (g) D. Gimenez, J. A. Aguilar, E. H. C. Bromley, S. L. Cobb, S. *Angew. Chemie Int. Ed*., 2018, **57**, 10549. (h) A. W. Wijaya, A. I. Nguyen, L. T. Roe, G. L. Butterfoss, R. K. Spencer, N. K. Li, R. N. Zuckermann, *J. Am. Chem. Soc*. 2019, **141**, 19436.

6 (a) N. H. Shah, G. L. Butterfoss, K. Nguyen, B. Yoo, R. Bonneau, D. L. Rabenstein, K. Kirshenbaum, *J. Am. Chem. Soc*., 2008, **130**, 16622. (b) J. R. Stringer, J. Aaron Crapster, I. A. Guzei, H. E. Blackwell, *J. Org. Chem*., 2010, **75**, 6068. (c) B. Paul, G. L. Butterfoss, M. G. Boswell, P. D. Renfrew, F. G. Yeung, N. H. Shah, C. Wolf, R. Bonneau, K. Kirshenbaum, *J. Am. Chem. Soc*., 2011, **133**, 10910. (d) J. A. Crapster, J. R. Stringer, I. A. Guzei, H. E. Blackwell, *Biopolymers* 2011, **96**, 604. (e) P. A. Jordan, B. Paul, G. L. Butterfoss, P. D. Renfrew, R. Bonneau, K. Kirshenbaum, *Biopolymers* 2011, **96**, 617. (f) B. Kanta Sarma, M. Yousufuddin, T. Kodadek, *Chem. Commun*., 2011, **47**, 10590. (g) B. K. Sarma, T. Kodadek, *ACS Comb. Sci*., 2012, **14**, 558. (h) C. M. Davern, B. D. Lowe, A. Rosfi, E. A. Ison, C. Proulx, *Chem. Sci*., 2021, **12**, 8401. (i) M. Pypec, L. Jouffret, C. Taillefumier and O. Roy, *Beilstein J. Org. Chem*.,2022, **18**, 845.

7 O. Roy, C. Caumes, Y. Esvan, C. Didierjean, S. Faure and C. Taillefumier, *Org. Lett.*, 2013, **15**, 2246.

8 G. Angelici, N. Bhattacharjee, O. Roy, S. Faure, C. Didierjean, L. Jouffret, F. Jolibois, L. Perrin and C. Taillefumier, *Chem. Commun.*, 2016, **52**, 4573.

9 (a) O. Roy, G. Dumonteil, S. Faure, L. Jouffret, A. Kriznik and C. Taillefumier, *J. Am. Chem. Soc.*, 2017, **139**, 13533. (b) M. Rzeigui, M. Traikia, L. Jouffret, A. Kriznik, J. Khiari, O. Roy and C. Taillefumier, *J. Org. Chem.*, 2020, **85**, 2190.

10 R. Shyam, L. Nauton, G. Angelici, O. Roy, C. Taillefumier and S. Faure, *Biopolymers*, 2019, **110**, e23273.

11 B. C. Hamper, S. A. Kolodziej, A. M. Scates, R. G. Smith, E. Cortez, *J. Org. Chem*., 1998, **63**, 708.

12 C. Baldauf, R. Günther and H.-J. Hofmann, *Phys. Biol.*, 2006, **3**, S1–S9.

13 S. W. Shuey, W. J. Delaney, M. C. Shah and M. A. Scialdone, *Bioorganic Med. Chem. Lett.*, 2006, **16**, 1245.

14 C. A. Olsen, M. Lambert, M. Witt, H. Franzyk and J. W. Jaroszewski, *Amino Acids*, 2008, **34**, 465.

15 C. A. Olsen, *Biopolymers*, 2011, **96**, 561.

16 G. Martelli, A. Monsignori, M. Orena, S. Rinaldi, N. Castellucci and C. Tomasini, *Amino Acids*, 2012, **43**, 2005.

17 J. S. Laursen, J. Engel-Andreasen, P. Fristrup, P. Harris and C. A. Olsen, *J. Am. Chem. Soc.*, 2013, **135**, 2835.

18 P. Sauerberg, J. P. Mogensen, L. Jeppesen, P. S. Bury, J. Fleckner, G. S. Olsen, C. B. Jeppesen, E. M. Wulff, P. Pihera, M. Havranek, Z. Polivka and I. Pettersson, *Bioorganic Med. Chem. Lett.*, 2007, **17**, 3198.

19 J. S. Laursen, J. Engel-Andreasen and C. A. Olsen, *Acc. Chem. Res.*, 2015, **48**, 2696.

20 J. S. Laursen, P. Harris, P. Fristrup and C. A. Olsen, *Nat. Commun.*, 2015, **6**, 7013.

21 I. Wellhöfer, K. Frydenvang, S. Kotesova, A. M. Christiansen, J. S. Laursen and C. A. Olsen, *J. Org. Chem.*, 2019, **84**, 3762.

22 C. Caumes, C. Fernandes, O. Roy, T. Hjelmgaard, E. Wenger, C. Didierjean, C. Taillefumier and S. Faure, *Org. Lett.*, 2013, **15**, 3626.

23 P. J. Stevenson, Org. Biomol. Chem., 2011, **9**, 2078.

24 J. C. Phillips, R. Braun, W. Wang, J. Gumbart, E. Tajkhorshid, E. Villa, C. Chipot, R. D. Skeel, L. Kalé and K. Schulten, *J. Comput. Chem.*, 2005, **26**, 1781.

25 J. Wang, R. M. Wolf, J. W. Caldwell, P. A. Kollman and D. A. Case, *J. Comput. Chem.*, 2004, **25**, 1157.

26 GaussView, Version 5, R. Dennington, T. Keith, and J. Millam, 2009. *Semichem Inc*., Shawnee Mission, KS

27 A. Crapster, I. A. Guzei, and H. E. Blackwell, *Angew. Chem. Int. Ed*., 2013, **52**, 1.